

Open quantum systems with nonlinear environmental backactions: Extended dissipaton theory versus core–system hierarchy construction

Zi-Hao Chen, Yao Wang,^{a)} Rui-Xue Xu,^{b)} and YiJing Yan

Hefei National Research Center for Physical Sciences at the Microscale and Department of Chemical Physics,
University of Science and Technology of China, Hefei, Anhui 230026, China

(Dated: 25 January 2023)

In this paper, we present a comprehensive account of quantum dissipation theories with the quadratic environment couplings. The theoretical development includes the Brownian solvation mode embedded hierarchical quantum master equations, a core–system hierarchy construction that verifies the extended dissipaton equation of motion (DEOM) formalism [R. X. Xu *et al.*, *J. Chem. Phys.* **148**, 114103 (2018)]. Developed are also the quadratic imaginary–time DEOM for equilibrium and the $\lambda(t)$ -DEOM for nonequilibrium thermodynamics problems. Both the celebrated Jarzynski equality and Crooks relation are accurately reproduced, which in turn confirms the rigorosity of the extended DEOM theories. While the extended DEOM is more numerically efficient, the core–system hierarchy quantum master equation is favorable for “visualizing” the correlated solvation dynamics.

I. INTRODUCTION

Quantum dissipation plays a crucial role in many fields of modern science, where irreversibility takes place during relaxation, dephasing, transport and thermodynamic processes.^{1–12} In these studies, the environmental non-Markovian and non-perturbative quantum nature would be prominent if the system and bath are strongly correlated. Various exact methods, such as the Feynman–Vernon influence functional approach¹³ and its differential equivalence, the hierarchical equations of motion (HEOM) formalism,^{14–22} had been constructed. There are also quite a few studies that treat HEOM as quantum Fokker–Planck (FP) type equations, via transferring the involving degrees of freedom into the Wigner representation, such as the quantum hierarchical FP equation.^{23–28} Besides, transformations from HEOM to the low–temperature quantum FP or Smoluchowski equations are also suggested.^{29,30} However, most of these theories are exact only for Gaussian environments with linear couplings. This linearity intrinsically implies a weak backaction of the central system on the surroundings.

On the other hand, the nonlinear system–bath interactions are generally common and appealing in real physical systems.^{31–40} The quest of an exact treatment of quantum dissipation with nonlinear environment couplings remains a challenging task in recent years.^{41–46} In this account, we consider the total system–plus–bath composite Hamiltonian to take the form of

$$H_{\tau} = H_s + h_b + \hat{Q}_s(\alpha_0 + \alpha_1 \hat{x}_b + \alpha_2 \hat{x}_b^2). \quad (1)$$

Here, H_s is the system Hamiltonian and \hat{Q}_s is the dissipative mode which can be an arbitrary Hermitian system operator. The bath Hamiltonian and solvation coordinate are

$$h_b = \frac{1}{2} \sum_j \omega_j (\hat{p}_j^2 + \hat{q}_j^2) \quad \text{and} \quad \hat{x}_b = \sum_j c_j \hat{q}_j, \quad (2)$$

respectively, where the Gaussian h_b is in line with the central limiting statistics description. The solvation coordinate \hat{x}_b is defined to be the linear part, but involved in both the α_1 and α_2 terms. In Eq. (1), \hat{Q}_s and \hat{x}_b are set to be dimensionless, while the α -parameters are of energy unit. When $\alpha_2 = 0$, it is reduced to the linear bath coupling case. The nonlinearity is exemplified here with the quadratic coupling. The approaches presented later in this account can all be extended to higher orders. Throughout this paper we set $\hbar = 1$ and $\beta = 1/(k_B T)$, with k_B being the Boltzmann constant and T the temperature.

To simulate the dynamics governed by the Hamiltonian in Eqs. (1) with (2), we had previously adopted the dissipaton theory. The dissipaton theory introduces statistical quasi-particles, dissipatons, to characterize the interacting bath statistical properties.^{47–51} The resulting dissipaton equation of motion (DEOM) is not only identical to the HEOM for the reduced system dynamics, but also convenient to treat the hybridized bath dynamics.^{51–53} Based on the DEOM, we had proposed two distinct approaches for the nonlinear bath coupling, namely, the extended DEOM^{41,42} and the stochastic-fields–dressed DEOM (SFD–DEOM).⁵⁴

In this work, an exact core–system hierarchy construction is developed. It explicitly treats the solvation phase space, including the nonlinear coupling term (α_2 term). We name it as the Brownian solvation mode embedded hierarchical quantum master equations (BSM–HQME), with the standard FP algebra^{55–57} being exploited. We further scrutinize the extended DEOM^{41,42} and the SFD–DEOM,⁵⁴ with the newly developed BSM–HQME. All of them agree with each other, as inferred from their theoretical constructions and also evident from numerical simulations. This implies the extended DEOM and the underlying generalized Wick’s theorem (GWT-2)^{41,42} are universally correct.

Some features of these methods are as follows. (i) The SFD–DEOM is exact in principle, constructed on the basis of SFD total Hamiltonian with only linear bath coupling terms, while the nonlinear terms are resolved via the stochastic fields. However, the SFD–DEOM approach is numerically available only for short–time evolutions, but subject to long–time instability. (ii) The BSM–HQME explicitly treats the solvation coordinate and momentum. Its phase space dynamics

^{a)}Electronic mail: wy2010@ustc.edu.cn

^{b)}Electronic mail: rxxu@ustc.edu.cn

can be directly computed using this approach. Taking the electron transfer process, for example, this approach provides the exact reaction coordinate evolutions. (iii) The extended DEOM is mostly numerically efficient among those three methods. It can be readily extended to imaginary-time (*i*-DEOM) formulations^{51,58,59} to compute the hybridization free energy. (iv) We can also develop the nonequilibrium λ -DEOM (neq- λ -DEOM)^{51,60} to investigate the fluctuation theorems, such as Jarzynski equality and Crooks relation. The results here in turn confirm the rigorousness of the extended DEOM theories.

The remainder of this paper is organized as follows. Section II comprises a complete description of extended DEOM. In Sec. III A, the BSM-HQME is developed in detail. The FP algebra is outlined in Appendix. The numerical cross-check is carried out among BSM-HQME, extended DEOM, and SFD-DEOM in terms of both real-dynamics and spectroscopies in Sec. III B. The explicit solvation mode dynamics are also computed using the BSM-HQME. Section IV is concerned with the system-bath thermodynamic mixing with nonlinear environment couplings. The Jarzynski equality and Crooks relation are accurately reproduced with extended DEOM for quadratic bath couplings. We summarize this work in Sec. V.

II. THE EXTENDED DEOM FORMALISM

In this section, we briefly review the extended DEOM formalism in Refs. 41 and 42 for nonlinear bath couplings. Before that, we first introduce the associated bath statistics. With the bath Hamiltonian and coupling in the form of Eqs. (1) and (2), the bath influence is completely described via the bath spectral density,

$$J(\omega \geq 0) = \frac{\pi}{2} \sum_j c_j^2 \delta(\omega - \omega_j) = -J(-\omega). \quad (3)$$

It is expressed in terms of $J(\omega) \equiv \text{Im}\chi_B(\omega)$, with^{1,4}

$$\chi_B(\omega) = i \int_0^\infty dt e^{i\omega t} \langle [\hat{x}_B(t), \hat{x}_B(0)] \rangle_B. \quad (4)$$

Here, $[\cdot, \cdot]$ denotes a commutator, $\hat{x}_B(t) \equiv e^{ih_B t} \hat{x}_B e^{-ih_B t}$ and $\langle \hat{O} \rangle_B \equiv \text{tr}_B(\hat{O} e^{-\beta h_B}) / \text{tr}_B e^{-\beta h_B}$. The fluctuation-dissipation theorem in relation to Eq. (4) reads^{1,4}

$$\langle \hat{x}_B(t) \hat{x}_B(0) \rangle_B = \frac{1}{\pi} \int_{-\infty}^\infty d\omega \frac{e^{-i\omega t} J(\omega)}{1 - e^{-\beta\omega}}. \quad (5)$$

This bare-bath subspace relation holds in general, regardless of the nature of bare bath Hamiltonian and also independent of the system-bath couplings involved in Eq. (1).

The DEOM formalism is established by expressing the influence of environment with a finite number of statistically independent quasi-particles, the dissipatons.^{21,47} We expand Eq. (5) in an exponential series,^{4,61,62}

$$\langle \hat{x}_B(t) \hat{x}_B(0) \rangle_B = \sum_{k=1}^K \eta_k e^{-\gamma_k t}. \quad (6)$$

Its time reversal is expressed in the form of^{4,63}

$$\langle \hat{x}_B(0) \hat{x}_B(t) \rangle_B = \langle \hat{x}_B(t) \hat{x}_B(0) \rangle_B^* = \sum_{k=1}^K \eta_k^* e^{-\gamma_k t}, \quad (7)$$

with \bar{k} being defined via $\gamma_{\bar{k}} \equiv \gamma_k^*$, which must also appear in Eq. (6). The solvation coordinate can then be recast in the dissipatons decomposition form,^{21,47}

$$\hat{x}_B = \sum_{k=1}^K \hat{f}_k, \quad (8)$$

with

$$\langle \hat{f}_k(t) \hat{f}_{k'}(0) \rangle_B = \langle \hat{f}_k \hat{f}_{k'} \rangle_B^> e^{-\gamma_k t} = \delta_{kk'} \eta_k e^{-\gamma_k t}, \quad (9a)$$

$$\langle \hat{f}_{k'}(0) \hat{f}_k(t) \rangle_B = \langle \hat{f}_{k'} \hat{f}_k \rangle_B^< e^{-\gamma_k t} = \delta_{kk'} \eta_k^* e^{-\gamma_k t}. \quad (9b)$$

Apparently, both Eqs. (6) and (7) are reproduced.

Dynamical variables in DEOM are the dissipaton density operators (DDOs):^{21,47}

$$\rho_{\mathbf{n}}^{(n)}(t) \equiv \rho_{n_1 \dots n_K}^{(n)}(t) \equiv \text{tr}_B [(\hat{f}_K^{n_K} \dots \hat{f}_1^{n_1})^\circ \rho_\tau(t)]. \quad (10)$$

The reduced system density operator is just $\rho_s(t) \equiv \rho_{\mathbf{0}}^{(0)}(t)$. The indexes $\mathbf{n} \equiv \{n_1 \dots n_K\}$ and $n = n_1 + \dots + n_K$ specify the occupations and the total number of dissipatons, respectively. The notation, $(\dots)^\circ$, denotes the irreducible representation. We have $(\hat{f}_k \hat{f}_{k'})^\circ = (\hat{f}_{k'} \hat{f}_k)^\circ$ for bosonic dissipatons.

The construction of DEOM starts from

$$\dot{\rho}_{\mathbf{n}}^{(n)}(t) \equiv \dot{\rho}_{n_1 \dots n_K}^{(n)}(t) \equiv \text{tr}_B [(\hat{f}_K^{n_K} \dots \hat{f}_1^{n_1})^\circ \dot{\rho}_\tau(t)], \quad (11)$$

with the total composite density operator satisfying

$$\dot{\rho}_\tau(t) = -i[H_\tau, \rho_\tau(t)]. \quad (12)$$

The dissipaton formalism consists of the generalized diffusion equation and the generalized Wick's theorems (GWTs). The former reads

$$\text{tr}_B \left[\left(\frac{\partial \hat{f}_k}{\partial t} \right)_B \rho_\tau(t) \right] = -\gamma_k \text{tr}_B [\hat{f}_k \rho_\tau(t)]. \quad (13)$$

It together with $\left(\frac{\partial \hat{f}_k}{\partial t} \right)_B = -i[\hat{f}_k, h_B]$ will give rise to

$$i \text{tr}_B \{ (\hat{f}_K^{n_K} \dots \hat{f}_1^{n_1})^\circ [h_B, \rho_\tau] \} = \left(\sum_{k=1}^K n_k \gamma_k \right) \rho_{\mathbf{n}}^{(n)}. \quad (14)$$

The GWT-1 evaluates the linear bath coupling with one dissipaton added each time. It reads^{21,47}

$$\begin{aligned} & \text{tr}_B [(\hat{f}_K^{n_K} \dots \hat{f}_1^{n_1})^\circ \hat{f}_\kappa \rho_\tau(t)] \\ &= \rho_{\mathbf{n}_\kappa^\pm}^{(n+1)}(t) + \sum_{k=1}^K n_k \langle \hat{f}_k \hat{f}_\kappa \rangle_B^> \rho_{\mathbf{n}_\kappa^-}^{(n-1)}(t). \end{aligned} \quad (15)$$

The expression of $\text{tr}_B [(\hat{f}_K^{n_K} \dots \hat{f}_1^{n_1})^\circ \rho_\tau(t) \hat{f}_\kappa]$ is similar, but with $\langle \hat{f}_k \hat{f}_\kappa \rangle_B^>$ being replaced by $\langle \hat{f}_\kappa \hat{f}_k \rangle_B^<$. The associated index \mathbf{n}_κ^\pm differs from $\mathbf{n} \equiv \{n_1 \dots n_K\}$ by replacing the specified n_k with $n_k \pm 1$. This specifies the $(n \pm 1)$ -particle DDO,

$\rho_{\mathbf{n}_k^\pm}^{(n\pm 1)}(t)$, in Eq.(15). In comparison, we may recall some properties about the ‘‘normal order’’ in textbooks, which arranges creation operators before annihilation operators. Denote this also with $(\cdot)^\circ$, such that $(\hat{a}^\dagger \hat{a})^\circ = (\hat{a} \hat{a}^\dagger)^\circ = \hat{a}^\dagger \hat{a}$. Assume $\hat{f} = \sqrt{\eta}(\hat{a} + \hat{a}^\dagger)$, with η being an arbitrary real parameter. It is easy to obtain $(\hat{f}^n)^\circ \hat{f} = (\hat{f}^{n+1})^\circ + n\eta(\hat{f}^{n-1})^\circ = \hat{f}(\hat{f}^n)^\circ$, in line with the standard normal ordering.⁶⁴ The GWT-1 is just the generalization of this result, which has been already verified analytically in the linear environmental coupling scenarios.^{51,65}

The GWT-2 is related to the quadratic bath coupling, where a pair of dissipatons are added each time. It was validated under the minimum–dissipaton ansatz,^{57,66} via the Zusman or the Fokker–Planck algebra.⁴¹ One of the purposes of this work is to confirm the GWT-2 beyond these limitations. More precisely, we will first assume the correctness of the GWT-2 in more general scenarios, and then scrutinize it numerically by comparing with the exact results from the SFD–DEOM⁵⁴ and the newly developed BSM–HQME (cf. Sec. III). In this sense, the GWT-2 is a validated ‘‘theorem’’ that is generally correct. However, a rigorous proof of GWT-2 within the canonical Feynman–Vernon influence functional formalism is absent so far. The GWT-2 is evaluated as^{41,42}

$$\begin{aligned} & \text{tr}_B [(\hat{f}_K^{n_K} \cdots \hat{f}_1^{n_1})^\circ (\hat{f}_K \hat{f}_{K'}) \rho_T(t)] \\ &= \rho_{\mathbf{n}_{KK'}^{(n+2)}}(t) + \langle \hat{f}_K \hat{f}_{K'} \rangle_B \rho_{\mathbf{n}}^{(n)}(t) + \sum_k n_k \langle \hat{f}_k \hat{f}_{K'} \rangle_B^> \rho_{\mathbf{n}_{KK'}^{(n)}}(t) \\ &+ \sum_k n_k \langle \hat{f}_k \hat{f}_K \rangle_B^> \rho_{\mathbf{n}_{kk'}^{(n)}}(t) \\ &+ \sum_{k,k'} n_k (n_{k'} - \delta_{kk'}) \langle \hat{f}_k \hat{f}_K \rangle_B^> \langle \hat{f}_{k'} \hat{f}_{K'} \rangle_B^> \rho_{\mathbf{n}_{kk'}^{(n-2)}}(t). \end{aligned} \quad (16)$$

The associated DDO index, $\mathbf{n}_{kk'}^{\pm\pm}$, differs from $\mathbf{n} \equiv n_1 \cdots n_K$ on the specified subindexes, n_k and $n_{k'}$, that are replaced by $n_k \pm 1$ and $n_{k'} \pm 1$, respectively. Together with Eqs. (8) and (9), we obtain

$$\begin{aligned} & \text{tr}_B [(\hat{f}_K^{n_K} \cdots \hat{f}_1^{n_1})^\circ \hat{x}_B^2 \rho_T(t)] \\ &= \sum_{kk'} \rho_{\mathbf{n}_{kk'}^{(n+2)}}(t) + \langle \hat{x}_B^2 \rangle_B \rho_{\mathbf{n}}^{(n)}(t) + 2 \sum_{kk'} n_k \eta_k \rho_{\mathbf{n}_{kk'}^{(n)}}(t) \\ &+ \sum_{kk'} n_k (n_{k'} - \delta_{kk'}) \eta_k \eta_{k'} \rho_{\mathbf{n}_{kk'}^{(n-2)}}(t). \end{aligned} \quad (17)$$

The expression of $\text{tr}_B [(\hat{f}_K^{n_K} \cdots \hat{f}_1^{n_1})^\circ \rho_T(t) \hat{x}_B^2]$ is similar, but with η_k and $\eta_{k'}$ being replaced by η_k^* and $\eta_{k'}^*$, respectively.

Combining Eqs. (11)–(17), the extended DEOM is finally constructed^{41,42}

$$\begin{aligned} \dot{\rho}_{\mathbf{n}}^{(n)} &= - \left(i\mathcal{L}_S + \sum_k n_k \eta_k \right) \rho_{\mathbf{n}}^{(n)} - i \left(\alpha_0 + \alpha_2 \langle \hat{x}_B^2 \rangle_B \right) \mathcal{A} \rho_{\mathbf{n}}^{(n)} \\ &- i\alpha_1 \sum_k \left(\mathcal{A} \rho_{\mathbf{n}_k^+}^{(n+1)} + n_k \mathcal{E}_k \rho_{\mathbf{n}_k^-}^{(n-1)} \right) - 2i\alpha_2 \sum_{kk'} n_k \mathcal{E}_k \rho_{\mathbf{n}_{kk'}^{(n)}} \\ &- i\alpha_2 \sum_{kk'} \left[\mathcal{A} \rho_{\mathbf{n}_{kk'}^{(n+2)}} + n_k (n_{k'} - \delta_{kk'}) \mathcal{B}_{kk'} \rho_{\mathbf{n}_{kk'}^{(n-2)}} \right], \end{aligned} \quad (18)$$

with $\mathcal{L}_S \hat{O} \equiv [H_S, \hat{O}]$ and other involved superoperators defined

as

$$\mathcal{A} \hat{O} \equiv [\hat{Q}_S, \hat{O}], \quad (19a)$$

$$\mathcal{B}_{kk'} \hat{O} \equiv \eta_k \eta_{k'}^* \hat{Q}_S \hat{O} - \eta_k^* \eta_{k'} \hat{O} \hat{Q}_S, \quad (19b)$$

$$\mathcal{E}_k \hat{O} \equiv \eta_k \hat{Q}_S \hat{O} - \eta_k^* \hat{O} \hat{Q}_S. \quad (19c)$$

III. BSM–HQME: A CORE–SYSTEM HIERARCHY CONSTRUCTION

In this section, we propose a new exact core–system hierarchy method, named as BSM–HQME. In the core–system description, the bath Hamiltonian of Eq. (2) is divided into two parts, the solvation mode and the secondary bath coupled to it. The FP algebra is used to provide a basis set for describing the solvation mode inside the core system.^{55–57} The details of BSM–HQME construction are given in Sec. III A. In Sec. III B, we carry out the numerical cross check among BSM–HQME, extended DEOM, and SFD–DEOM. Both dynamics and spectroscopies are simulated, together with the explicit solvation mode dynamics obtained from the BSM–HQME.

A. The construction of BSM–HQME

In the core–system description, the bath Hamiltonian of Eq. (2) is divided into the solvation modes and secondary bath parts with the Caldeira–Leggett model, which reads

$$h_B = \frac{1}{2} \omega_B (\hat{p}_B^2 + \hat{x}_B^2) + \frac{1}{2} \sum_j \tilde{\omega}_j [\hat{p}_j^2 + (\tilde{x}_j - \frac{\tilde{c}_j}{\tilde{\omega}_j} \hat{x}_B)^2]. \quad (20)$$

The solvation mode behaves as a Brownian oscillator, with the correlation function, $\langle \hat{x}_B(t) \hat{x}_B(0) \rangle_B$, given by Eq. (5) in which^{56,57}

$$J(\omega) = \text{Im} \frac{\omega_B}{\omega_B^2 - \omega^2 - i\omega \zeta_B(\omega)}. \quad (21)$$

Here, $\zeta_B(\omega) \equiv \int_0^\infty dt e^{i\omega t} \tilde{\zeta}_B(t)$, with the classical friction function reading

$$\tilde{\zeta}_B(t) = \omega_B \sum_j (\tilde{c}_j^2 / \tilde{\omega}_j) \cos(\tilde{\omega}_j t). \quad (22)$$

The spectral density of the secondary bath, $\tilde{h}_B = \frac{1}{2} \sum_j \tilde{\omega}_j (\hat{p}_j^2 + \hat{x}_j^2)$, is then^{56,57}

$$\tilde{J}(\omega) = \frac{\omega}{\omega_B} \text{Re} \zeta_B(\omega), \quad (23)$$

and the secondary bath fluctuation–dissipation theorem reads

$$\langle \tilde{F}(t) \tilde{F} \rangle_{\tilde{B}} = \frac{1}{\pi} \int_{-\infty}^\infty d\omega \frac{\tilde{J}(\omega) e^{-i\omega t}}{1 - e^{-\beta\omega}} \quad (24)$$

where $\langle \hat{O} \rangle_{\tilde{B}} \equiv \text{tr}_{\tilde{B}} (\hat{O} e^{-\beta h_B}) / \text{tr}_{\tilde{B}} e^{-\beta h_B}$.

Using Eq.(24) with Eq.(23), we can write down the HEOM/DEOM where the primary system and solvation mode compose the core system,

$$H_{\text{core}} = H_s + \hat{Q}_s F(\hat{x}_B) + \frac{\omega_B}{2} (\hat{p}_B^2 + \hat{x}_B^2) + \tilde{\lambda} \hat{x}_B^2 \quad (25)$$

where

$$F(\hat{x}_B) = \alpha_0 + \alpha_1 \hat{x}_B + \alpha_2 \hat{x}_B^2 \quad (26)$$

and

$$\tilde{\lambda} \equiv \frac{1}{2} \sum_j \frac{\tilde{c}_j^2}{\tilde{\omega}_j} = \frac{\tilde{\zeta}_B(0)}{2\omega_B}. \quad (27)$$

The secondary bath is treated as the environment. According to Eq. (24), followed by applying the exponential decomposition scheme,^{61,62,67} we obtain

$$\langle \tilde{F}(t) \tilde{F}(0) \rangle_{\tilde{B}} = \sum_{k=1}^K \tilde{\eta}_k e^{-\tilde{\gamma}_k t} \quad (t > 0) \quad (28)$$

The HEOM for the core system can be then constructed as

$$\begin{aligned} \dot{\rho}_{\tilde{\mathbf{n}}} = & -(i\mathcal{L}_{\text{core}} + \gamma_{\tilde{\mathbf{n}}})\rho_{\tilde{\mathbf{n}}} - i \sum_{k=1}^K \hat{x}_B^\times \rho_{\tilde{\mathbf{n}}_k^+} \\ & - i \sum_{k=1}^K \tilde{\eta}_k (\tilde{\eta}_k \hat{x}_B^> - \tilde{\eta}_k^* \hat{x}_B^<) \rho_{\tilde{\mathbf{n}}_k^-}, \end{aligned} \quad (29)$$

where $\mathcal{L}_{\text{core}} \hat{O} \equiv [H_{\text{core}}, \hat{O}]$ and $\gamma_{\tilde{\mathbf{n}}} = \sum_k \tilde{\eta}_k \tilde{\gamma}_k$. The $\tilde{\mathbf{n}}$ is the array of dissipaton occupation numbers; see comments after Eq. (10). Hereafter, we denote $A^\times \equiv A^> - A^<$, $A^> \hat{O} \equiv A \hat{O}$, and $A^< \hat{O} \equiv \hat{O} A$. In Eq. (29), $\{\rho_{\tilde{\mathbf{n}}}\}$ are the DDOs of the core system, i.e. the primary system plus the solvation mode degrees of freedom. Let $\hat{W}_{\tilde{\mathbf{n}}}(x_B, p_B) \equiv (\rho_{\tilde{\mathbf{n}}})_{\text{Wigner}}$ be the Wigner representation of the solvation subspace. Moreover, we expand $\{\hat{W}_{\tilde{\mathbf{n}}}(x_B, p_B)\}$ by the FP basis set as [cf. Eq. (A.18)]

$$\begin{aligned} \hat{W}_{\tilde{\mathbf{n}}}(x_B, p_B; t) = & \left(\frac{\beta \omega_B}{2\pi} \right)^{\frac{1}{2}} \sum_{n_1, n_2} \frac{s_{n_1, n_2}}{\sqrt{n_1! n_2!}} \rho_{n_1, n_2; \tilde{\mathbf{n}}}(t) \\ & \times e^{-\frac{\beta \omega_B}{4} (x_B^2 + p_B^2)} \Psi_{n_1, n_2}(x_B, p_B). \end{aligned} \quad (30)$$

Here, $\{\rho_{n_1, n_2; \tilde{\mathbf{n}}}\}$ are operators in the original system subspace, and $\rho_{00; \tilde{\mathbf{n}}}$ is just the reduced system operator. The scaling parameters, $\{s_{n_1, n_2}\}$, and the functions $\{\Psi_{n_1, n_2}\}$ are detailed in Appendix. After some simple algebra, we obtain $\rho_{\tilde{\mathbf{n}}; \tilde{\mathbf{n}}} \equiv \rho_{n_1, n_2; \tilde{\mathbf{n}}}$ the EOM,

$$\begin{aligned} \dot{\rho}_{\tilde{\mathbf{n}}; \tilde{\mathbf{n}}} = & -(i\mathcal{L}_{\text{core}} + \gamma_{\tilde{\mathbf{n}}})\rho_{\tilde{\mathbf{n}}; \tilde{\mathbf{n}}} - i \sum_{k=1}^{N_K} \hat{x}_B^\times \rho_{\tilde{\mathbf{n}}; \tilde{\mathbf{n}}_k^+} \\ & - i \sum_{k=1}^{N_K} \tilde{\eta}_k (\tilde{\eta}_k \hat{x}_B^> \rho_{\tilde{\mathbf{n}}; \tilde{\mathbf{n}}_k^-} - \tilde{\eta}_k^* \hat{x}_B^< \rho_{\tilde{\mathbf{n}}; \tilde{\mathbf{n}}_k^-}). \end{aligned} \quad (31)$$

The solvation mode actions, \hat{x}_B^\times and \hat{x}_B^\times are considered in the Wigner representation; see Eqs. (A.24a)–(A.24d). Moreover,

$$\begin{aligned} \mathcal{L}_{\text{core}} \rho_{\tilde{\mathbf{n}}; \tilde{\mathbf{n}}} = & \mathcal{L}_s \rho_{\tilde{\mathbf{n}}; \tilde{\mathbf{n}}} + \hat{Q}_s F(\hat{x}_B^>) \rho_{\tilde{\mathbf{n}}; \tilde{\mathbf{n}}} - F(\hat{x}_B^<) \rho_{\tilde{\mathbf{n}}; \tilde{\mathbf{n}}} \hat{Q}_s \\ & + \frac{\omega_B}{2} (\hat{p}_B^>^2 + \hat{x}_B^>^2 - \hat{p}_B^<^2 - \hat{x}_B^<^2) \rho_{\tilde{\mathbf{n}}; \tilde{\mathbf{n}}} \\ & + \tilde{\lambda} (\hat{x}_B^>^2 - \hat{x}_B^<^2) \rho_{\tilde{\mathbf{n}}; \tilde{\mathbf{n}}}. \end{aligned} \quad (32)$$

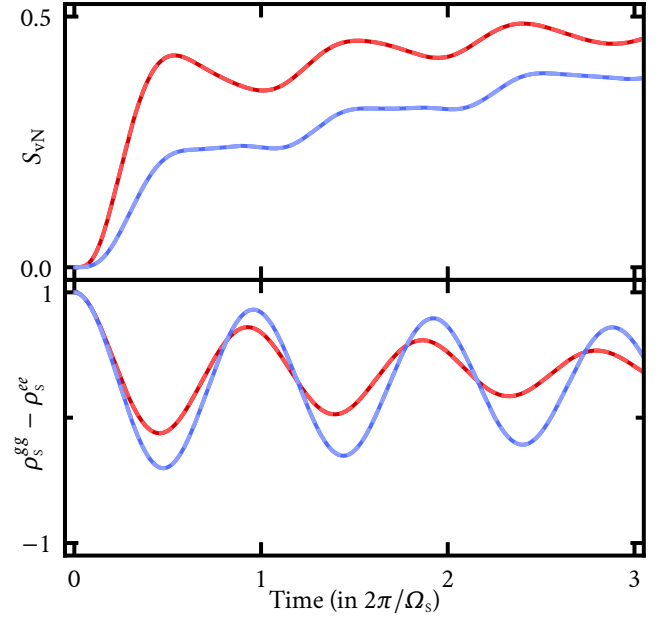


FIG. 1. Comparison between extended DEOM (solid) and BSM-HQME (dashed) in terms of von Neumann entropy, $S_{\text{vN}} = -\text{tr}_s(\rho_s \ln \rho_s)$, and the evolution of population, $\rho_s^{gg} - \rho_s^{ee}$. Here, we set $\omega_{eg} = V = \omega_B$. The Rabi frequency is $\Omega_s = \sqrt{5}\omega_B$. The bath related parameters are selected as $(\theta_B, \lambda/\omega_B) = (1.125, 0.1)$ and $(1.333, 0.25)$, plotted in blue and red curves, respectively.

The above solvation mode subspace Wigner representation also highlights the role of the FP formulation.^{41,55,68,69}

B. Numerical demonstrations

For demonstration, we select a two-state model system as in Ref. 42. In this model, the total Hamiltonian can be described by

$$H_T = h_g |g\rangle\langle g| + (h_e + \omega_{eg}) |e\rangle\langle e|, \quad (33)$$

where

$$h_e = \frac{1}{2} \omega_B (\hat{p}_B^2 + \hat{x}_B^2) + \frac{1}{2} \sum_k \tilde{\omega}_k \left[\tilde{p}_k^2 + \left(\tilde{x}_k - \frac{\tilde{c}_k}{\tilde{\omega}_k} \hat{x}_B \right)^2 \right], \quad (34)$$

and

$$h_g = \frac{1}{2} \omega_B' (\hat{p}_B'^2 + \hat{x}_B'^2) + \frac{1}{2} \sum_k \tilde{\omega}_k' \left[\tilde{p}_k'^2 + \left(\tilde{x}_k' - \frac{\tilde{c}_k'}{\tilde{\omega}_k'} \hat{x}_B' \right)^2 \right], \quad (35)$$

follow the Caldeira–Leggett’s interaction form.⁷⁰ Then in the H_g -based description, H_T can be reformulated as

$$\begin{aligned} H_T = & \omega_{eg} |e\rangle\langle e| + h_g + (h_e - h_g) |e\rangle\langle e| \\ = & \omega_{eg} |e\rangle\langle e| + h_g + (\alpha_0 + \alpha_1 \hat{x}_B + \alpha_2 \hat{x}_B^2) |e\rangle\langle e|, \end{aligned} \quad (36)$$

with

$$\alpha_0 = \lambda \theta_B^2, \quad \alpha_1 = -(2\lambda \omega_B)^{\frac{1}{2}} \theta_B^2, \quad \alpha_2 = \frac{\omega_B}{2} (\theta_B^2 - 1). \quad (37)$$

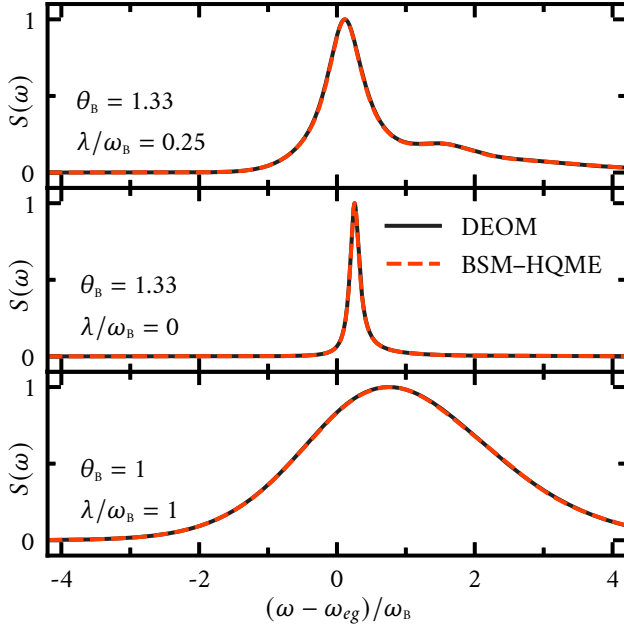


FIG. 2. Absorption spectra via the extended DEOM (black solid) and the BSM-HQME (red dashed). We set $\omega_{eg} = 50\omega_b$ and three pairs of the specified bath related parameters $(\theta_b, \lambda/\omega_b)$. Other parameters are the same as those in Fig. 1.

Here, λ represents the linear-displacement induced reorganization and $\theta_b = \omega'_b/\omega_b$. Both the linear and quadratic coupling strengths are determined by these two parameters. We adopt the Drude model for the secondary bath,

$$\zeta_b(\omega) = \frac{2i\tilde{\lambda}\omega_b}{\omega + i\tilde{\gamma}}, \quad (38)$$

with $\tilde{\lambda}$ being the reorganization energy defined in Eq. (27). The resulted $\tilde{J}(\omega)$ reads [cf. Eq. (23)]

$$\tilde{J}(\omega) = \frac{2\tilde{\lambda}\tilde{\gamma}\omega}{\omega^2 + \tilde{\gamma}^2}. \quad (39)$$

We set $\tilde{\lambda} = 5\omega_b$, $\tilde{\gamma} = 15\omega_b$ and $\beta\omega_b = 1$, with ω_b being the unit in the following demonstrations.

Figure 1 shows the extended DEOM dynamics, in comparison with the BSM-HQME results, on the von Neumann entropy (upper panel) and the population (lower panel). We assume the system Hamiltonian as $H_s = \omega_{eg}|e\rangle\langle e| + V(|e\rangle\langle g| + |g\rangle\langle e|)$ and the initial state being the equilibrium ground state in the absence of nonadiabatic coupling ($V = 0$). As seen from the figure, the extended DEOM results agree perfectly with those of the BSM-HQME. We also carry out the SFD-DEOM⁵⁴ calculation with the parameters $(\theta_b, \lambda/\omega_b) = (1.125, 0.1)$. The converged results (not shown in the figure) also match those of both BSM-HQME and extended DEOM. The SFD-DEOM encounters error accumulation in the long-time simulation, requiring a vast of trajectories to converge when α_2 is relatively large. In the BSM-HQME simulations, we exploit the on-the-fly numerical filter technique,⁷¹ with

the accuracy of 10^{-8} that effectively corresponds to the converged level of truncation at $n_1 + n_2 = 8$ and $\sum_k \tilde{n}_k = 30$.

Figure 2 reports the evaluated absorption spectra using the extended DEOM and the BSM-HQME, with three pairs of the specified bath parameters $(\theta_b, \lambda/\omega_b)$. The absorption spectrum is defined as

$$S(\omega) = \text{Re} \int_0^\infty dt e^{i\omega t} \langle \hat{\mu}_s(t) \hat{\mu}_s(0) \rangle \quad (40)$$

with $\hat{\mu}_s = |e\rangle\langle g| + |g\rangle\langle e|$. As shown in the figure, the extended DEOM and BSM-HQME agree with each other perfectly.

Figure 3 (Multimedia view) depicts the time evolution of the solvation mode phase-space distribution [cf. Eq. (30) with Eqs. (A.21) and (A.22)],

$$\rho_B(x_B, p_B; t) \equiv \text{tr}_S [W_{\hat{0}}(x_B, p_B; t)]. \quad (41)$$

We choose $(\theta_b, \lambda/\omega_b) = (1, 0.25)$, $(1.33, 0)$ and $(1.33, 0.25)$ to represent the pure linear (L), the pure quadratic (Q) and the mixed (L+Q) coupling bath scenarios, respectively. The video shows the dynamic interplay between the nonadiabatic coupling V , the linear bath coupling that contributes to the center displacement, and the quadratic bath coupling that causes the curvature change. Evidently, compared to the DEOM, the BSM-HQME is the choice to “visualize” the solvation mode dynamics.

IV. THERMODYNAMIC MIXING

In this section, we extend the present DEOM formalism to thermodynamics problems. Involved would be the imaginary-time DEOM (*i*-DEOM) and also nonequilibrium λ -DEOM (neq- λ -DEOM), to be detailed in Sec. IV A and Sec. IV B, respectively. The key quantities are the system-bath mixing free-energy, nonequilibrium work and its distribution function. The numerical results in Sec. IV C reproduce the Jarzynski equality⁷² and the Crooks relation.⁷³

A. Extended *i*-DEOM formalism

The *i*-DEOM aims at the hybridization partition function,

$$Z_{\text{hyb}} \equiv Z_\tau / Z_0 \equiv \text{Tr} \varrho_\tau(\beta), \quad (42)$$

with $Z_\tau \equiv \text{Tr} e^{-\beta H_\tau}$ and $Z_0 \equiv \text{Tr} e^{-\beta H_0}$, where $H_0 = H_s + h_B$ [cf. Eq. (1)]. The hybridization free-energy before and after isotherm system-bath mixing, $A_{\text{hyb}}(T) \equiv A_\tau(T) - A_0(T)$, is given by

$$A_{\text{hyb}}(T) = -\beta^{-1} \ln Z_{\text{hyb}}(T). \quad (43)$$

This is to be evaluated by using Eq. (42) via

$$\varrho_\tau(\tau) = e^{-\tau H_\tau} e^{-(\beta-\tau)H_0} / Z_0, \quad (44)$$

that satisfies

$$\frac{d\varrho_\tau(\tau)}{d\tau} = -(H_s^\times + h_B^\times + H_{\text{SB}}^\times) \varrho_\tau(\tau), \quad (45)$$

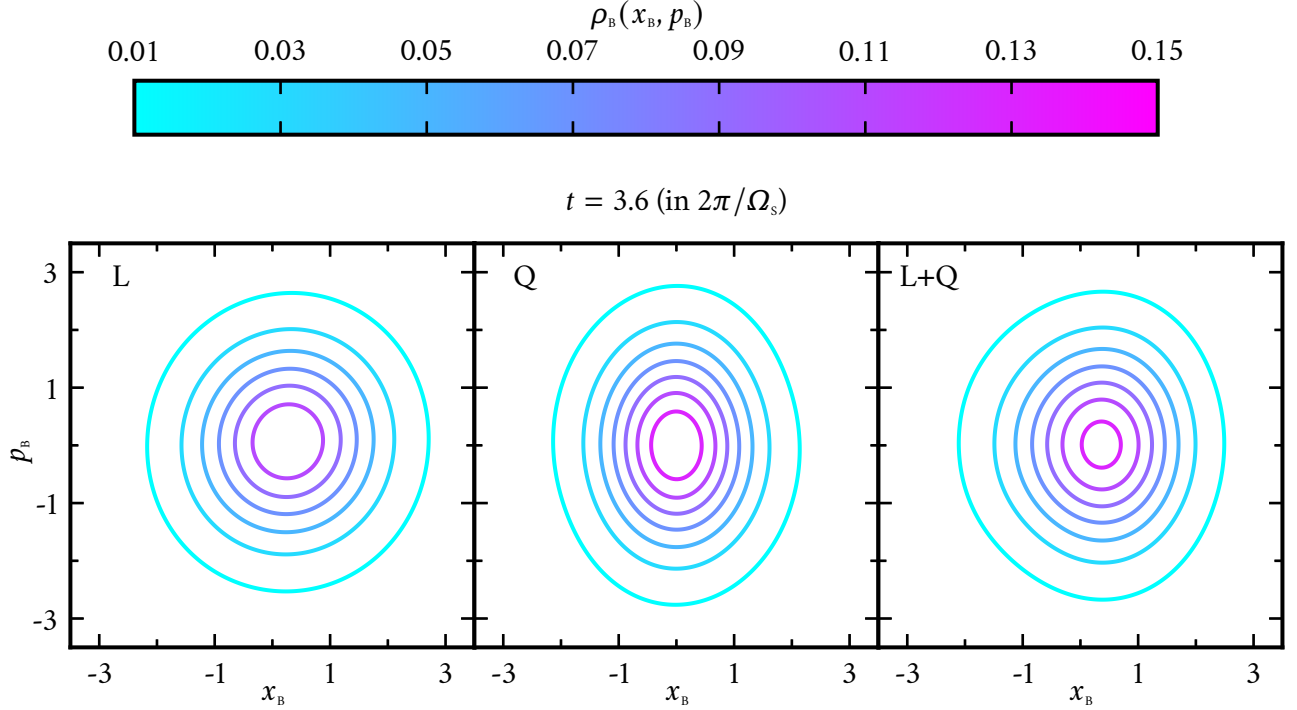


FIG. 3. Phase space dynamics of solvation mode evaluated via BSM-HQME with $(\theta_b, \lambda/\omega_b) = (1, 0.25)$, $(1.33, 0)$ and $(1.33, 0.25)$, representing the pure linear (L), the pure quadratic (Q) and the mixed (L+Q) coupling bath scenarios. Other parameters are the same as those in Fig. 1. (Multimedia view)

where $H_{\text{SB}} \equiv \hat{Q}_s(\alpha_0 + \alpha_1 \hat{x}_b + \alpha_2 \hat{x}_b^2)$. The i -DEOM–space mapping goes by^{51,58}

$$\varrho_{\tau}(\tau) \rightarrow \varrho(\tau) \equiv \{\varrho_{\mathbf{n}}^{(n)}(\tau)\}. \quad (46)$$

We obtain^{51,58}

$$\frac{d\varrho_{\mathbf{n}}^{(n)}(\tau)}{d\tau} = -\varrho_{\mathbf{n}}^{(n)}(\tau; H_s^{\times}) - \varrho_{\mathbf{n}}^{(n)}(\tau; h_b^{\times}) - \varrho_{\mathbf{n}}^{(n)}(\tau; H_{\text{SB}}^{\times}) \quad (47)$$

with

$$\begin{aligned} \varrho_{\mathbf{n}}^{(n)}(\tau; H_{\text{SB}}^{\times}) &= \alpha_0 \hat{Q}_s \varrho_{\mathbf{n}}^{(n)}(\tau) + \alpha_1 \hat{Q}_s \varrho_{\mathbf{n}}^{(n)}(\tau; \hat{x}_b^{\times}) \\ &+ \alpha_2 \hat{Q}_s \varrho_{\mathbf{n}}^{(n)}(\tau; \hat{x}_b^{\times 2}). \end{aligned} \quad (48)$$

In parallel to the dissipaton algebra introduced in Sec. II, especially Eq. (17) that deal with the quadratic coupling, we obtain the final i -DEOM formalism,

$$\begin{aligned} \dot{\varrho}_{\mathbf{n}}^{(n)} &= \left(-\mathcal{L}_s + i \sum_k n_k \gamma_k \right) \varrho_{\mathbf{n}}^{(n)} - (\alpha_0 + \alpha_2 \langle \hat{x}_b^2 \rangle_B) \mathcal{A} \varrho_{\mathbf{n}}^{(n)} \\ &- \alpha_1 \sum_k \left(\mathcal{A} \varrho_{\mathbf{n}_k^+}^{(n+1)} + n_k \mathcal{C}_k \varrho_{\mathbf{n}_k^-}^{(n-1)} \right) - 2\alpha_2 \sum_{kk'} n_k \mathcal{C}_k \varrho_{\mathbf{n}_{kk'}}^{(n)} \\ &- \alpha_2 \sum_{kk'} \left[\mathcal{A} \varrho_{\mathbf{n}_{kk'}^+}^{(n+2)} + n_k (n_{k'} - \delta_{kk'}) \mathcal{B}_{kk'} \varrho_{\mathbf{n}_{kk'}^-}^{(n-2)} \right], \end{aligned} \quad (49)$$

with

$$\mathcal{A} \hat{\mathcal{O}} \equiv \hat{Q}_s \hat{\mathcal{O}}, \quad \mathcal{C}_k \hat{\mathcal{O}} \equiv \eta_k \hat{Q}_s \hat{\mathcal{O}}. \quad (50a)$$

$$\mathcal{B}_{kk'} \hat{\mathcal{O}} \equiv \eta_k \eta_{k'} \hat{Q}_s \hat{\mathcal{O}}. \quad (50b)$$

Evidently, when $\alpha_2 = 0$, Eq. (49) reduces to the conventional i -DEOM formalism.^{51,58} The solutions of $Z_{\text{hyb}} = \text{Tr} \varrho_{\mathbf{0}}^{(0)}(\beta)$ can be obtained by propagation of Eq. (49) from the initial values $\varrho_{\mathbf{0}}^{(0)}(0) = e^{-\beta H_0}/Z_0$ and $\varrho_{\mathbf{n}}^{(n>0)}(0) = 0$.

B. Extended neq- λ -DEOM formalism

Turn to the neq- λ -DEOM formalism, aiming at the system–bath mixing nonequilibrium work and its distribution function.^{51,60} The involved $\lambda(t)$ –augmented total composite Hamiltonian reads

$$H_{\tau}(t) = H_s + h_b + \lambda(t) H_{\text{SB}}. \quad (51)$$

A time–dependent mixing function $\lambda(t)$ is used subject to $\lambda(t=0) = 0$ and $\lambda(t=t_f) = 1$. This represents a nonequilibrium scenario. In related studies, the work distribution $p(w)$ is the key quantity. There exists the Jarzynski equality⁷²

$$\langle e^{-\beta w} \rangle \equiv \int_{-\infty}^{\infty} dw e^{-\beta w} p(w) = e^{-\beta A_{\text{hyb}}} \quad (52)$$

and the Crooks relation⁷³

$$e^{-\beta w} p(w) = e^{-\beta A_{\text{hyb}}} \bar{p}(-w). \quad (53)$$

The latter is about a pair of conjugate processes, with the forward and backward processes being controlled by $\lambda(t)$

and $\bar{\lambda}(t) \equiv \lambda(t_f - t)$, respectively.⁷⁴ The forward work distribution $p(w)$ and the backward $\bar{p}(-w)$ cross at $w = A_{\text{hyb}}$ where A_{hyb} can be obtained via the i -DEOM calculation with Eqs. (42) and (43).

The neq- λ -DEOM enables the accurate evaluation of $p(w)$. To proceed, we start with $H_0|n\rangle = H_T(\lambda = 0)|n\rangle = \varepsilon_n|n\rangle$ and $H_T(\lambda = 1)|N\rangle = E_N|N\rangle$ before and after mixing. The distribution of mixing work is given by⁷⁵

$$p(w) = \sum_{N,n} \delta(w - E_N + \varepsilon_n) P_{N,n}(t_f, 0) e^{-\beta \varepsilon_n} / Z_0. \quad (54)$$

In Eq. (54), $P_{N,n}(t, 0) = |\langle N | \hat{U}_T(t) | n \rangle|^2$ is the transition probability with the propagator $\hat{U}_T(t)$ being governed by the Hamiltonian $H_T(t) = H_0 + \lambda(t) H_{\text{SB}}$.

Define then

$$\hat{\Phi}_T(t; \tau) = \hat{U}_T(t) \hat{V}_+(t; \tau) \rho_0^{\text{eq}}(T) \hat{V}_-(t; \tau) \hat{U}_T^\dagger(t), \quad (55)$$

where

$$\hat{V}_\pm(t; \tau) = \exp_\pm \left[\frac{i\tau}{2} \int_0^t dt' \lambda(t') H_{\text{SB}} \right]. \quad (56)$$

It can be shown that^{75,76}

$$p(w) = \frac{1}{2\pi} \int_{-\infty}^{\infty} d\tau e^{-i w \tau} \text{Tr} \hat{\Phi}_T(t_f; \tau). \quad (57)$$

This concludes that $\hat{\Phi}_T(t; \tau)$, defined in Eq. (55), is the work generating operator, satisfying

$$\frac{\partial \hat{\Phi}_T}{\partial t} = -i[H_S^\times + h_B^\times + \lambda_-(t) H_{\text{SB}}^\times - \lambda_+(t) H_{\text{SB}}^\times] \hat{\Phi}_T, \quad (58)$$

with

$$\lambda_\pm(t) \equiv \lambda(t) \pm (\tau/2) \dot{\lambda}(t). \quad (59)$$

Initially, $\hat{\Phi}_T(0; \tau) = \rho_0^{\text{eq}}(T) = e^{-\beta H_0} / Z_0$, as inferred from Eq. (55).

Similar to Eq. (46), we obtain the dissipations-augmented work generating operators (D-WGOs) mapping,

$$\hat{\Phi}_T(t; \tau) \rightarrow \hat{\Phi}(t; \tau) \equiv \{\hat{\Phi}_n^{(n)}(t; \tau)\}. \quad (60)$$

Following the similar procedure from Eq. (12) to Eq. (18) applied to Eq. (58), we obtain the D-WGO correspondence.^{51,60}

$$\begin{aligned} \dot{\Phi}_n^{(n)} = & - \left(i \mathcal{L}_S + \sum_k n_k \gamma_k \right) \Phi_n^{(n)} - i \left(\alpha_0 + \alpha_2 \langle \hat{x}_B^2 \rangle_B \right) \mathcal{A}(t) \Phi_n^{(n)} \\ & - i \alpha_1 \sum_k \left[\mathcal{A}(t) \Phi_{n_k^+}^{(n+1)} + n_k \mathcal{C}_k(t) \Phi_{n_k^-}^{(n-1)} \right] \\ & - i \alpha_2 \sum_{kk'} \left[\mathcal{A}(t) \Phi_{n_{kk'}^{++}}^{(n+2)} + n_k (n_{k'} - \delta_{kk'}) \tilde{\mathcal{B}}_{kk'}(t) \Phi_{n_{kk'}^{--}}^{(n-2)} \right] \\ & - 2i \alpha_2 \sum_{kk'} n_k \tilde{\mathcal{C}}_k(t) \Phi_{n_{kk'}^{+-}}^{(n)}, \end{aligned} \quad (61)$$

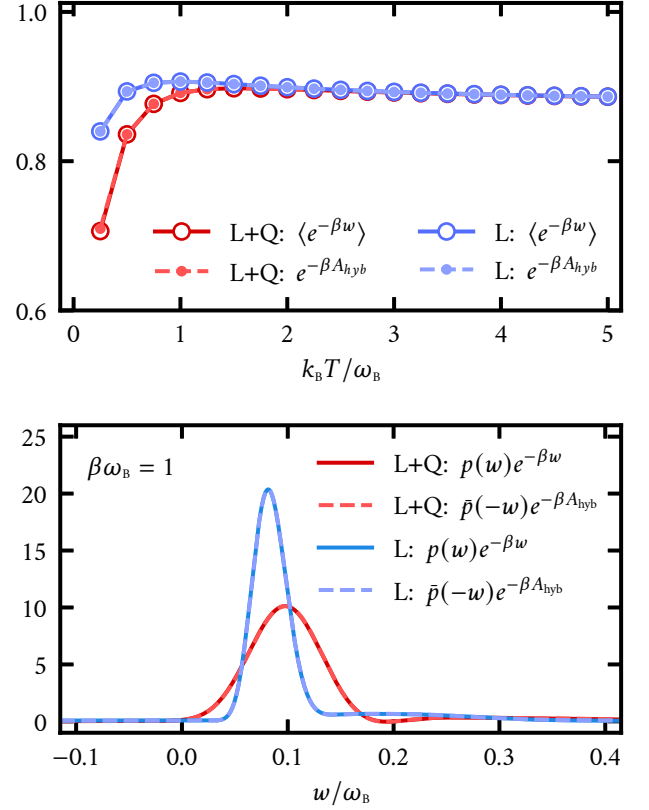


FIG. 4. The results of DEOM with GWT-2, in terms of the Jarzynski equality (upper panel) and the Crooks relation (lower panel). Parameters are the same as those of Fig. 3.

where

$$\mathcal{A}(t) \hat{O} \equiv \lambda_-(t) \hat{Q}_S \hat{O} - \lambda_+(t) \hat{O} \hat{Q}_S, \quad (62a)$$

$$\tilde{\mathcal{B}}_{kk'}(t) \hat{O} \equiv \lambda_-(t) \eta_k \eta_{k'} \hat{Q}_S \hat{O} - \lambda_+(t) \eta_k^* \eta_{k'}^* \hat{O} \hat{Q}_S, \quad (62b)$$

$$\tilde{\mathcal{C}}_k(t) \hat{O} \equiv \lambda_-(t) \eta_k \hat{Q}_S \hat{O} - \lambda_+(t) \eta_k^* \hat{O} \hat{Q}_S. \quad (62c)$$

In relation to $\hat{\Phi}_T(0; \tau) = \rho_0^{\text{eq}}(T) = e^{-\beta H_0} / Z_0$, the initial values to Eq. (61) are

$$\hat{\Phi}_0^{(0)}(0; \tau) = e^{-\beta H_S} / Z_S \quad \text{and} \quad \hat{\Phi}_n^{(n>0)}(0; \tau) = 0. \quad (63)$$

Finally, by using Eq. (61) with Eqs. (62) and (59), we evaluate

$$p(w) = \frac{1}{2\pi} \int_{-\infty}^{\infty} d\tau e^{-i w \tau} \text{tr}_S [\hat{\Phi}_0^{(0)}(t_f; \tau)]. \quad (64)$$

C. Numerical demonstrations

In our simulations, we set the forward and backward time-dependent mixing function to be

$$\lambda(t) = \frac{1 - e^{-at}}{1 - e^{-at_f}}, \quad (65)$$

and

$$\bar{\lambda}(t) = \lambda(t_f - t) = \frac{e^{at_f} - e^{at}}{e^{at_f} - 1}, \quad (66)$$

respectively. Figure 4 reports the DEOM results in terms of the Jarzynski equality (52) and the Crooks relation (53). The $e^{-\beta A_{\text{hyb}}}$ and the w related functions are evaluated by the methods described in Sec. IV A and Sec. IV B, respectively. Numerical simulations are carried out with the same setup as in Fig. 3. The upper panel shows that the Jarzynski equality is recovered. At the high-temperature regime, the classical equipartition theorem holds as seen from the coincidence between the results of L and L+Q scenarios. The lower panel reproduces the Crooks relation. The resulting work distribution function can be used in analyzing the cumulants of various orders, including the center, the variance, the skewness and so on.⁷⁷ It is worth reemphasizing that Fig. 4 in turn confirms the rigorousness of the extended DEOM theories, covering the real-time, the imaginary-time and the nonequilibrium $\lambda(t)$ dynamics.

V. SUMMARY

To conclude, we present a comprehensive account of extended DEOM with quadratic environments, which could in principle be generalized to arbitrary nonlinear bath coupling scenarios. The developments include also an equivalent core-system phase-space hierarchy construction, BSM-HQME, as verified both theoretically and numerically. The extended DEOM is numerically more efficient, whereas the core-system BSM-HQME is favorable for “visualizing” the correlated solvation dynamics.

While the present theories are elaborated with the single dissipative mode case, the extensions to multiple dissipative modes, including modes mixing (i.e. Duschinsky rotation), are straightforward. Moreover, the existing system-bath entanglement theorem with linear environment coupling^{51,58,78,79} can be further investigated with the inclusion of quadratic environment coupling. The aforementioned theoretical developments would comprise required toolkits for the construction of practical dissipaton-correlated coarse-graining molecular dynamics and thermodynamics methods.

It is also worth noting that the GWTs are validated within the canonical Feynman-Vernon influence functional formalism with the linear environmental couplings.⁶⁵ However, it is rather cumbersome to prove the GWTs and derive the EOM in nonlinear coupling scenarios using the Feynman-Vernon influence functional approach. There is no simple analytical expression of nonlinear influence functionals. On the other hand, the dissipaton algebra enables the GWT-2 in the most direct manner. The resulting Eq. (18), the extended DEOM formalism,^{41,42} is numerically validated by comparing with other two very different approaches, BSM-HQME and SFD-DEOM, in this work. This indicates that the dissipaton theory would be an important building block towards the future development of open quantum systems.

ACKNOWLEDGMENTS

Support from the Ministry of Science and Technology of China (Grant No. 2021YFA1200103) and the National Natural Science Foundation of China (Grant Nos. 22103073 and 22173088) is gratefully acknowledged.

Appendix: Onset of algebra for Brownian solvation mode

1. The Fokker-Planck operator and basis set construction

The following part is the procedure to generate the FP basis set for describing the solvation mode inside the core system. Let us start from Eq. (5) with Eq. (21). In the Markovian limit, $\zeta_{\text{B}}(\omega) = \zeta_{\text{B}}$, by further adopting the high-temperature approximation,⁵⁷ we have

$$\langle \hat{x}_{\text{B}}(t) \hat{x}_{\text{B}}(0) \rangle_{\text{B}} \approx \eta_{+} e^{-\gamma_{+} t} + \eta_{-} e^{-\gamma_{-} t}, \quad (\text{A.1})$$

with

$$\gamma_{\pm} = \frac{1}{2} [\zeta_{\text{B}} \pm (\zeta_{\text{B}}^2 - 4\omega_{\text{B}}^2)^{\frac{1}{2}}], \quad (\text{A.2})$$

and

$$\eta_{\pm} = \mp \frac{\omega_{\text{B}}}{\gamma_{+} - \gamma_{-}} \left(\frac{1}{\beta \gamma_{\pm}} - \frac{i}{2} \right). \quad (\text{A.3})$$

It should be noticed that the Markovian and high-temperature limits are needed only for the construction of FP operator and FP algebra, which are *not* necessary for the BSM-HQME, which is exact at any temperature.

Then one may construct the FP operator \mathcal{L}_{FP} that would generate the FP basis set,⁵⁵⁻⁵⁷

$$\begin{aligned} \mathcal{L}_{\text{FP}}(\cdot) \equiv & i \frac{\omega_{\text{B}}}{2} [\hat{p}_{\text{B}}^2 + \hat{x}_{\text{B}}^2, \cdot] + \frac{\zeta_{\text{B}}}{\beta \omega_{\text{B}}} [\hat{x}_{\text{B}}, [\hat{x}_{\text{B}}, \cdot]] \\ & + i \frac{\zeta_{\text{B}}}{2} [\hat{x}_{\text{B}}, \{\hat{p}_{\text{B}}, \cdot\}]. \end{aligned} \quad (\text{A.4})$$

In Wigner representation, the FP operator, Eq. (A.4), can be converted to a solvation phase-space operator as

$$L_{\text{FP}} \equiv \omega_{\text{B}} \left(\frac{\partial}{\partial x_{\text{B}}} p_{\text{B}} - \frac{\partial}{\partial p_{\text{B}}} x_{\text{B}} \right) - \frac{\zeta_{\text{B}}}{\beta \omega_{\text{B}}} \frac{\partial^2}{\partial p_{\text{B}}^2} - \zeta_{\text{B}} \frac{\partial}{\partial p_{\text{B}}} p_{\text{B}}, \quad (\text{A.5})$$

where x_{B} and p_{B} are c-number valued solvation coordinate and momentum, respectively. Under the similarity transformation

$$\tilde{L}_{\text{FP}} \equiv e^S L_{\text{FP}} e^{-S}, \quad (\text{A.6})$$

with $S \equiv \frac{\beta \omega_{\text{B}}}{4} (x_{\text{B}}^2 + p_{\text{B}}^2)$, we can recast \tilde{L}_{FP} as

$$\begin{aligned} \tilde{L}_{\text{FP}} = & \omega_{\text{B}} (a_2^{\dagger} a_1 - a_1^{\dagger} a_2) + \zeta_{\text{B}} a_2^{\dagger} a_2, \\ = & \gamma_{+} c_1^{\dagger} c_1^{-} + \gamma_{-} c_2^{\dagger} c_2^{-}. \end{aligned} \quad (\text{A.7})$$

The first line involves solvation phase–space operators,

$$\begin{aligned} a_1 &= \frac{\sqrt{\beta\omega_B}}{2}x_B + \frac{1}{\sqrt{\beta\omega_B}}\frac{\partial}{\partial x_B}, \\ a_2 &= \frac{\sqrt{\beta\omega_B}}{2}p_B + \frac{1}{\sqrt{\beta\omega_B}}\frac{\partial}{\partial p_B}, \end{aligned} \quad (\text{A.8a})$$

and the corresponding

$$\begin{aligned} a_1^\dagger &= \frac{\sqrt{\beta\omega_B}}{2}x_B - \frac{1}{\sqrt{\beta\omega_B}}\frac{\partial}{\partial x_B}, \\ a_2^\dagger &= \frac{\sqrt{\beta\omega_B}}{2}p_B - \frac{1}{\sqrt{\beta\omega_B}}\frac{\partial}{\partial p_B}. \end{aligned} \quad (\text{A.8b})$$

In Eq. (A.7), the ω_B –term describes the coherent dynamics and the ζ_B –term is responsible for dissipation. The second line describes the quasi-particle diagonalization, with

$$\begin{aligned} c_1^- &\equiv r_2 a_1 + r_1 a_2, & c_2^- &\equiv r_1 a_1 + r_2 a_2, \\ c_1^+ &\equiv -r_2 a_1^\dagger + r_1 a_2^\dagger, & c_2^+ &\equiv r_1 a_1^\dagger - r_2 a_2^\dagger, \end{aligned} \quad (\text{A.9})$$

and

$$r_1 \equiv \sqrt{\gamma_+ / (\gamma_+ - \gamma_-)}, \quad r_2 \equiv \sqrt{\gamma_- / (\gamma_+ - \gamma_-)}. \quad (\text{A.10})$$

Note that $c_{1,2}^+ \neq (c_{1,2}^-)^\dagger$. It is easy to verify that they satisfy the bosonic commutation relations as

$$\begin{aligned} [c_j^-, c_{j'}^+] &= [a_j, a_{j'}^\dagger] = \delta_{jj'}, \\ [c_j^\pm, c_{j'}^\pm] &= [a_j, a_{j'}] = [a_j^\dagger, a_{j'}^\dagger] = 0. \end{aligned} \quad (\text{A.11})$$

The eigenfunctions of \tilde{L}_{FP} can now be obtained as

$$\Psi_{n_1, n_2}(x_B, p_B) = \frac{1}{\sqrt{n_1! n_2!}} (c_1^+)^{n_1} (c_2^+)^{n_2} \Psi_{00}(x_B, p_B), \quad (\text{A.12})$$

with

$$\Psi_{00}(x_B, p_B) \equiv \left(\frac{\beta\omega_B}{2\pi}\right)^{\frac{1}{2}} e^{-\frac{\beta\omega_B}{4}(x_B^2 + p_B^2)}. \quad (\text{A.13})$$

It can be verified that

$$\tilde{L}_{\text{FP}} \Psi_{n_1, n_2} = (n_1 \gamma_+ + n_2 \gamma_-) \Psi_{n_1, n_2}. \quad (\text{A.14})$$

Furthermore, by denoting $\tilde{c}_j^\pm \equiv (c_j^\mp)^\dagger$, we can also construct the eigenfunctions $\{\tilde{\Psi}_{n_1, n_2}\}$ of $\tilde{L}_{\text{FP}}^\dagger$ in a similar way, reading

$$\tilde{\Psi}_{n_1, n_2}(x_B, p_B) = \frac{1}{\sqrt{n_1! n_2!}} (\tilde{c}_1^+)^{n_1} (\tilde{c}_2^+)^{n_2} \Psi_{00}(x_B, p_B), \quad (\text{A.15})$$

satisfying

$$\tilde{L}_{\text{FP}}^\dagger \tilde{\Psi}_{n_1, n_2} = (n_1 \gamma_+^* + n_2 \gamma_-^*) \tilde{\Psi}_{n_1, n_2}. \quad (\text{A.16})$$

The functions $\{\tilde{\Psi}_{n_1, n_2}\}$ are orthonormal with respect to $\{\Psi_{n_1, n_2}\}$ as

$$\iint dx_B dp_B \tilde{\Psi}_{n_1, n_2}^*(x_B, p_B) \Psi_{n'_1, n'_2}(x_B, p_B) = \delta_{n_1 n'_1} \delta_{n_2 n'_2}. \quad (\text{A.17})$$

Any function $W(x_B, p_B)$, including that of Eq. (30), can be expanded under this set of eigenfunctions $\{\Psi_{n_1, n_2}\}$ as

$$\begin{aligned} W(x_B, p_B) &= \left(\frac{\beta\omega_B}{2\pi}\right)^{\frac{1}{2}} \sum_{n_1, n_2} \frac{s_{n_1, n_2}}{\sqrt{n_1! n_2!}} \rho_{n_1, n_2} \\ &\times e^{-\frac{\beta\omega_B}{4}(x_B^2 + p_B^2)} \Psi_{n_1, n_2}(x_B, p_B). \end{aligned} \quad (\text{A.18})$$

Here, the parameters

$$s_{n_1, n_2} \equiv (-1)^{n_1} (\beta\omega_B)^{\frac{n_1+n_2}{2}} r_2^{-n_1} r_1^{-n_2} \quad (\text{A.19})$$

are chosen for later convenience and $\{\rho_{n_1, n_2}\}$ are the coefficients. It should be noted that $\{\rho_{n_1, n_2}\}$ can be not necessarily c-numbers, but operators including other degrees of freedom. Inversely, using the orthonormal relation, Eq. (A.17), we have

$$\begin{aligned} \rho_{n_1, n_2} &= \frac{\sqrt{n_1! n_2!}}{s_{n_1, n_2}} \left(\frac{\beta\omega_B}{2\pi}\right)^{-\frac{1}{2}} \iint dx_B dp_B \tilde{\Psi}_{n_1, n_2}^*(x_B, p_B) \\ &\times e^{\frac{\beta\omega_B}{4}(x_B^2 + p_B^2)} W(x_B, p_B). \end{aligned} \quad (\text{A.20})$$

Moreover, the $\Psi_{n_1, n_2}(x_B, p_B)$ can be explicitly expressed via Eq. (A.12) with Eqs. (A.8b) and (A.9), as

$$\begin{aligned} \Psi_{n_1, n_2}(x_B, p_B) &= \sum_{j_1, j_2} \binom{n_1}{j_1} \binom{n_2}{j_2} r_1^{n_2 - j_2 + j_1} (-r_2)^{n_1 - j_1 + j_2} \\ &\times \sqrt{\frac{(n_1 + n_2 - j_1 - j_2)! (j_1 + j_2)!}{n_1! n_2!}} \\ &\times \Psi_{n_1 + n_2 - j_1 - j_2}(x_B) \Psi_{j_1 + j_2}(p_B). \end{aligned} \quad (\text{A.21})$$

Here, the harmonic eigenfunctions, $\psi_n(z)$, read

$$\psi_n(z) \equiv \left(\frac{\beta\omega_B}{2\pi}\right)^{\frac{1}{4}} \frac{e^{-\frac{\beta\omega_B}{4}z^2}}{\sqrt{2^n n!}} H_n\left(\sqrt{\frac{\beta\omega_B}{2}}z\right) \quad (\text{A.22})$$

where $H_n(z)$ is the n th-order Hermitian polynomials. Thus we finish the procedure to generate the FP basis set, $\{\Psi_{n_1, n_2}\}$ [cf. Eq. (A.21)].

2. Actions of coordinate and momentum operators

In this subsection, we derive the actions of coordinate and momentum operators on $W(x_B, p_B)$ expressed in Eq. (A.18). Firstly we map the left/right actions of coordinate and momentum operators \hat{x}_B^\pm and \hat{p}_B^\pm into the Wigner representation as⁸⁰

$$\hat{x}_B^\pm \rightarrow x_B \pm \frac{i}{2} \frac{\partial}{\partial p_B} \quad \text{and} \quad \hat{p}_B^\pm \rightarrow p_B \mp \frac{i}{2} \frac{\partial}{\partial x_B}. \quad (\text{A.23})$$

Then by using Eq. (A.18), we obtain the solvation mode actions on ρ_{n_1, n_2} as

$$\hat{x}_B^>\rho_{n_1, n_2} = \rho_{n_1+1, n_2} + \rho_{n_1, n_2+1} + n_1\eta + \rho_{n_1-1, n_2} + n_2\eta - \rho_{n_1, n_2-1}, \quad (\text{A.24a})$$

$$\hat{x}_B^<\rho_{n_1, n_2} = \rho_{n_1+1, n_2} + \rho_{n_1, n_2+1} + n_1\bar{\eta}^* + \rho_{n_1-1, n_2} + n_2\bar{\eta}^* - \rho_{n_1, n_2-1}, \quad (\text{A.24b})$$

$$\omega_B \hat{p}_B^>\rho_{n_1, n_2} = -\gamma + \rho_{n_1+1, n_2} - \gamma - \rho_{n_1, n_2+1} - n_1\bar{\eta}^* - \gamma - \rho_{n_1-1, n_2} - n_2\bar{\eta}^* + \gamma + \rho_{n_1, n_2-1}, \quad (\text{A.24c})$$

$$\omega_B \hat{p}_B^<\rho_{n_1, n_2} = -\gamma + \rho_{n_1+1, n_2} - \gamma - \rho_{n_1, n_2+1} - n_1\eta - \gamma - \rho_{n_1-1, n_2} - n_2\eta + \gamma + \rho_{n_1, n_2-1}. \quad (\text{A.24d})$$

Here, we denote

$$\bar{\eta}_\pm^* \equiv \mp \frac{\omega_B}{\gamma_+ - \gamma_-} \left(\frac{1}{\beta\gamma_\pm} + \frac{i}{2} \right). \quad (\text{A.25})$$

The derivations of Eqs. (A.24a)–(A.24d) are as follows. Let us start with the actions of coordinate operator, \hat{x}_B , in the Wigner representation [cf. Eq. (A.18) with Eq. (A.8b)],

$$\begin{aligned} \hat{x}_B^\pm W(x_B, p_B) &= \left(x_B \pm \frac{i}{2} \frac{\partial}{\partial p_B} \right) W(x_B, p_B), \\ &= \left(\frac{\beta\omega_B}{2\pi} \right)^{\frac{1}{2}} \sum_{n_1, n_2} \frac{s_{n_1, n_2}}{\sqrt{n_1! n_2!}} \rho_{n_1, n_2} \left(x_B \pm \frac{i}{2} \frac{\partial}{\partial p_B} \right) \\ &\quad \times e^{-\frac{\beta\omega_B}{4}(x_B^2 + p_B^2)} \Psi_{n_1, n_2} \\ &= \left(\frac{\beta\omega_B}{2\pi} \right)^{\frac{1}{2}} \sum_{n_1, n_2} \frac{s_{n_1, n_2}}{\sqrt{n_1! n_2!}} \rho_{n_1, n_2} e^{-\frac{\beta\omega_B}{4}(x_B^2 + p_B^2)} \\ &\quad \times \left(\frac{a_1 + a_1^\dagger}{\sqrt{\beta\omega_B}} \mp \frac{i\sqrt{\beta\omega_B}}{2} a_2^\dagger \right) \Psi_{n_1, n_2}. \end{aligned}$$

Apply then Eq. (A.9) and the FP algebra,^{55,57} resulting in

$$\begin{aligned} \hat{x}_B^\pm W &= \left(\frac{\beta\omega_B}{2\pi} \right)^{\frac{1}{2}} \sum_{n_1, n_2} \frac{s_{n_1, n_2}}{\sqrt{n_1! n_2!}} \rho_{n_1, n_2} e^{-\frac{\beta\omega_B}{4}(x_B^2 + p_B^2)} \\ &\quad \times \frac{1}{\sqrt{\beta\omega_B}} \left[-r_2 c_1^- + r_1 c_2^- + (r_2 \mp ir_1 \beta\omega_B/2) c_1^+ \right. \\ &\quad \left. + (r_1 \mp ir_2 \beta\omega_B/2) c_2^+ \right] \Psi_{n_1, n_2} \\ &= \left(\frac{\beta\omega_B}{2\pi} \right)^{\frac{1}{2}} \sum_{n_1, n_2} \frac{s_{n_1, n_2}}{\sqrt{n_1! n_2!}} \rho_{n_1, n_2} e^{-\frac{\beta\omega_B}{4}(x_B^2 + p_B^2)} \\ &\quad \times \frac{1}{\sqrt{\beta\omega_B}} \left[-r_2 \sqrt{n_1} \Psi_{n_1-1, n_2} + r_1 \sqrt{n_2} \Psi_{n_1, n_2-1} \right. \\ &\quad \left. + (r_2 \mp ir_1 \beta\omega_B/2) \sqrt{n_1+1} \Psi_{n_1+1, n_2} \right. \\ &\quad \left. + (r_1 \mp ir_2 \beta\omega_B/2) \sqrt{n_2+1} \Psi_{n_1, n_2+1} \right] \\ &= \left(\frac{\beta\omega_B}{2\pi} \right)^{\frac{1}{2}} e^{-\frac{\beta\omega_B}{4}(x_B^2 + p_B^2)} \left[(1) + (2) + (3) + (4) \right], \end{aligned}$$

where

$$(1) = \sum_{n_1, n_2} \frac{s_{n_1+1, n_2}}{\sqrt{(n_1+1)! n_2!}} \rho_{n_1+1, n_2} \frac{-r_2}{\sqrt{\beta\omega_B}} \sqrt{n_1+1} \Psi_{n_1, n_2}$$

$$\begin{aligned} &= \sum_{n_1, n_2} \frac{s_{n_1, n_2}}{\sqrt{n_1! n_2!}} \rho_{n_1+1, n_2} \Psi_{n_1, n_2}. \\ (2) &= \sum_{n_1, n_2} \frac{s_{n_1, n_2+1}}{\sqrt{n_1! (n_2+1)!}} \rho_{n_1, n_2+1} \frac{r_1}{\sqrt{\beta\omega_B}} \sqrt{n_2+1} \Psi_{n_1, n_2} \\ &= \sum_{n_1, n_2} \frac{s_{n_1, n_2}}{\sqrt{n_1! n_2!}} \rho_{n_1, n_2+1} \Psi_{n_1, n_2}. \\ (3) &= \sum_{n_1, n_2} \frac{\sqrt{n_1} s_{n_1-1, n_2}}{\sqrt{(n_1-1)! n_2!}} \rho_{n_1-1, n_2} \left(\frac{r_2 \mp ir_1 \beta\omega_B/2}{\sqrt{\beta\omega_B}} \right) \Psi_{n_1, n_2} \\ &= \sum_{n_1, n_2} \frac{s_{n_1, n_2}}{\sqrt{n_1! n_2!}} \rho_{n_1-1, n_2} \left(\frac{-r_2^2}{\beta\omega_B} \pm \frac{ir_1 r_2}{2} \right) n_1 \Psi_{n_1, n_2} \\ &= \sum_{n_1, n_2} \frac{s_{n_1, n_2}}{\sqrt{n_1! n_2!}} \rho_{n_1-1, n_2} (\eta_+ / \bar{\eta}_+^*) n_1 \Psi_{n_1, n_2}. \\ (4) &= \sum_{n_1, n_2} \frac{\sqrt{n_2} s_{n_1, n_2-1}}{\sqrt{n_1! (n_2-1)!}} \rho_{n_1, n_2-1} \left(\frac{r_1 \mp ir_2 \beta\omega_B/2}{\sqrt{\beta\omega_B}} \right) \Psi_{n_1, n_2} \\ &= \sum_{n_1, n_2} \frac{s_{n_1, n_2}}{\sqrt{n_1! n_2!}} \rho_{n_1, n_2-1} \left(\frac{r_1^2}{\beta\omega_B} \mp \frac{ir_1 r_2}{2} \right) n_2 \Psi_{n_1, n_2} \\ &= \sum_{n_1, n_2} \frac{s_{n_1, n_2}}{\sqrt{n_1! n_2!}} \rho_{n_1, n_2-1} (\eta_- / \bar{\eta}_-^*) n_2 \Psi_{n_1, n_2}. \end{aligned}$$

In the last steps of above derivations, Eqs. (A.3) and (A.10) are used. We then finish deriving Eqs. (A.24a) and (A.24b) by adding the four terms together. Similarly, for actions of p_B^\pm on the coefficient function ρ_{n_1, n_2} , we obtain Eqs. (A.24c) and (A.24d).

Turn to core-system EOM in Eq. (31) with Eq. (32). By using Eqs. (A.24a)–(A.24d), we obtain

$$\begin{aligned} \dot{\rho}_{\mathbf{n}; \bar{\mathbf{n}}} &= - \left[i\mathcal{L}_S - 2(n_1 - n_2)\omega_B r_1 r_2 + \gamma_{\bar{\mathbf{n}}} \right. \\ &\quad \left. + i \sum_{j=1}^2 (2n_j + 1) (\tilde{\lambda} C_j + \alpha_2 \mathcal{C}_j) + i\alpha_0 \mathcal{A} \right] \rho_{\mathbf{n}; \bar{\mathbf{n}}} \\ &\quad - \sum_{j=1}^2 \left[(-1)^j n_j \omega_B r_1 r_2 (1 + \gamma_j / \gamma_j) \right. \\ &\quad \left. + 2in_j (\tilde{\lambda} C_j + \alpha_2 \mathcal{C}_j) \right] \rho_{\mathbf{n}_j^\pm; \bar{\mathbf{n}}} \\ &\quad - i\alpha_1 \sum_{j=1}^2 \left(\mathcal{A} \rho_{\mathbf{n}_j^\pm; \bar{\mathbf{n}}} + n_j \mathcal{C}_j \rho_{\mathbf{n}_j^\mp; \bar{\mathbf{n}}} \right) - i \sum_{j=1}^2 \sum_{k=1}^{N_K} n_j C_j \rho_{\mathbf{n}_j^\mp; \bar{\mathbf{n}}_k^\pm} \\ &\quad - i \sum_{j=1}^2 \sum_{k=1}^{N_K} \tilde{n}_k \left(C_k \rho_{\mathbf{n}_j^\pm; \bar{\mathbf{n}}_k^-} + n_j \tilde{B}_{jk} \rho_{\mathbf{n}_j^\mp; \bar{\mathbf{n}}_k^-} \right) \\ &\quad - i \sum_{j=1}^2 \sum_{j'=1}^2 n_j (n_{j'} - \delta_{jj'}) (\tilde{\lambda} B_{jj'} + \alpha_2 \mathcal{B}_{jj'}) \rho_{\mathbf{n}_{jj'}^\mp; \bar{\mathbf{n}}} \\ &\quad - i\alpha_2 \sum_{j=1}^2 \sum_{j'=1}^2 \mathcal{A} \rho_{\mathbf{n}_{jj'}^\pm; \bar{\mathbf{n}}}, \quad (\text{A.26}) \end{aligned}$$

with $\gamma_{1/2} = \gamma_\pm$ and $\tilde{\lambda}$ being given in Eq. (27),

$$\begin{aligned} B_{jj'} &= \eta_j \eta_{j'} - \bar{\eta}_j^* \bar{\eta}_{j'}^*, \quad C_j = \eta_j - \bar{\eta}_j^*, \\ \tilde{B}_{jk} &= \eta_j \bar{\eta}_k - \bar{\eta}_j^* \bar{\eta}_k^*, \quad \tilde{C}_k = \bar{\eta}_k - \bar{\eta}_k^*. \end{aligned} \quad (\text{A.27})$$

The involved superoperators are similar to those of Eq. (19),

but with

$$\begin{aligned}\mathcal{A}\hat{O} &= \hat{Q}_s\hat{O} - \hat{O}\hat{Q}_s, \quad \mathcal{C}_j\hat{O} = \eta_j\hat{Q}_s\hat{O} - \bar{\eta}_j^*\hat{O}\hat{Q}_s, \\ \mathcal{B}_{jj'}\hat{O} &= \eta_j\eta_{j'}\hat{Q}_s\hat{O} - \bar{\eta}_j^*\bar{\eta}_{j'}^*\hat{O}\hat{Q}_s.\end{aligned}\quad (\text{A.28})$$

Note also that $\bar{j} = 2$ when $j = 1$, and vice versa.

- ¹U. Weiss, *Quantum Dissipative Systems*, World Scientific, Singapore, 2021, 5th ed.
- ²H. Kleinert, *Path Integrals in Quantum Mechanics, Statistics, Polymer Physics, and Financial Markets*, World Scientific, Singapore, 5th edition, 2009.
- ³H. P. Breuer and F. Petruccione, *The Theory of Open Quantum Systems*, Oxford University Press, New York, 2002.
- ⁴Y. J. Yan and R. X. Xu, “Quantum mechanics of dissipative systems,” *Annu. Rev. Phys. Chem.* **56**, 187 (2005).
- ⁵A. Nitzan, *Chemical Dynamics in Condensed Phases: Relaxation, Transfer and Reactions in Condensed Molecular Systems*, Oxford University Press, New York, 2006.
- ⁶S. Mukamel, *The Principles of Nonlinear Optical Spectroscopy*, Oxford University Press, New York, 1995.
- ⁷W. H. Louisell, *Quantum Statistical Properties of Radiation*, Wiley, New York, 1973.
- ⁸F. Haake, “Statistical treatment of open systems by generalized master equations,” in *Quantum Statistics in Optics and Solid State Physics: Springer Tracts in Modern Physics, Vol. 66*, edited by G. Höhler, pages 98–168, Springer, Berlin, 1973.
- ⁹Y. Akamatsu, “Heavy quark master equations in the Lindblad form at high temperatures,” *Phys. Rev. D* **91**, 056002 (2015).
- ¹⁰V. Chernyak and S. Mukamel, “Collective coordinates for nuclear spectral densities in energy transfer and femtosecond spectroscopy of molecular aggregates,” *J. Chem. Phys.* **105**, 4565 (1996).
- ¹¹I. Imry, *Introduction to Mesoscopic Physics*, Oxford university press, 2002.
- ¹²H. Haug and A.-P. Jauho, *Quantum Kinetics in Transport and Optics of Semiconductors*, Springer-Verlag, Berlin, 2nd, substantially revised edition, 2008, Springer Series in Solid-State Sciences 123.
- ¹³R. P. Feynman and F. L. Vernon, Jr., “The theory of a general quantum system interacting with a linear dissipative system,” *Ann. Phys.* **24**, 118 (1963).
- ¹⁴Y. Tanimura, “Nonperturbative expansion method for a quantum system coupled to a harmonic-oscillator bath,” *Phys. Rev. A* **41**, 6676 (1990).
- ¹⁵Y. Tanimura, “Stochastic Liouville, Langevin, Fokker-Planck, and master equation approaches to quantum dissipative systems,” *J. Phys. Soc. Jpn.* **75**, 082001 (2006).
- ¹⁶Y. A. Yan, F. Yang, Y. Liu, and J. S. Shao, “Hierarchical approach based on stochastic decoupling to dissipative systems,” *Chem. Phys. Lett.* **395**, 216 (2004).
- ¹⁷R. X. Xu, P. Cui, X. Q. Li, Y. Mo, and Y. J. Yan, “Exact quantum master equation via the calculus on path integrals,” *J. Chem. Phys.* **122**, 041103 (2005).
- ¹⁸R. X. Xu and Y. J. Yan, “Dynamics of quantum dissipation systems interacting with bosonic canonical bath: Hierarchical equations of motion approach,” *Phys. Rev. E* **75**, 031107 (2007).
- ¹⁹J. S. Jin, X. Zheng, and Y. J. Yan, “Exact dynamics of dissipative electronic systems and quantum transport: Hierarchical equations of motion approach,” *J. Chem. Phys.* **128**, 234703 (2008).
- ²⁰L. Z. Ye, X. L. Wang, D. Hou, R. X. Xu, X. Zheng, and Y. J. Yan, “HEOM-QUICK: A program for accurate, efficient and universal characterization of strongly correlated quantum impurity systems,” *WIREs Comp. Mol. Sci.* **6**, 608 (2016).
- ²¹Y. J. Yan, J. S. Jin, R. X. Xu, and X. Zheng, “Dissipaton equation of motion approach to open quantum systems,” *Frontiers Phys.* **11**, 110306 (2016).
- ²²Y.-M. Yan, T. Xing, and Q. Shi, “A new method to improve the numerical stability of the hierarchical equations of motion for discrete harmonic oscillator modes,” *J. Chem. Phys.* **153**, 204109 (2020).
- ²³Y. Tanimura and P. G. Wolynes, “Quantum and classical Fokker-Planck equations for a Gaussian-Markovian noise bath,” *Phys. Rev. A* **43**, 4131 (1991).
- ²⁴Y. Tanimura and S. Mukamel, “Multistate quantum Fokker-Planck approach to nonadiabatic wave packet dynamics in pump-probe spectroscopy,” *J. Chem. Phys.* **101**, 3049 (1994).
- ²⁵Y. Tanimura and Y. Maruyama, “Gaussian-Markovian quantum Fokker-Planck approach to nonlinear spectroscopy of a displaced Morse potentials system: dissociation, predissociation, and optical Stark effects,” *J. Chem. Phys.* **107**, 1779 (1997).
- ²⁶T. Ikeda and Y. Tanimura, “Probing photoisomerization processes by means of multi-dimensional electronic spectroscopy: The multi-state quantum hierarchical Fokker-Planck equation approach,” *J. Chem. Phys.* **147**, 014102 (2017).
- ²⁷T. Ikeda and Y. Tanimura, “Low-Temperature Quantum Fokker-Planck and Smoluchowski Equations and Their Extension to Multistate Systems,” *J. Chem. Theory Comput.* **15**, 2517 (2019).
- ²⁸Y. Tanimura, “Real-time and imaginary-time quantum hierarchical Fokker-Planck equations,” *J. Chem. Phys.* **142**, 144110 (2015).
- ²⁹T.-C. Li, Y.-M. Yan, and Q. Shi, “A low-temperature quantum Fokker-Planck equation that improves the numerical stability of the hierarchical equations of motion for the Brownian oscillator spectral density,” *J. Chem. Phys.* **156**, 064107 (2022).
- ³⁰T. Ikeda and A. Nakayama, “Collective bath coordinate mapping of “hierarchy” in hierarchical equations of motion,” *J. Chem. Phys.* **156**, 104104 (2022).
- ³¹D. Vion, A. Aassime, A. Cottet, P. Joyez, H. Pothier, C. Urbina, D. Esteve, and M. H. Devoret, “Manipulating the quantum state of an electrical circuit,” *Science* **296**, 886 (2002).
- ³²Y. Makhlin and A. Shnirman, “Dephasing of solid-state qubits at optimal points,” *Phys. Rev. Lett.* **92**, 178301 (2004).
- ³³E. A. Muljarov and R. Zimmermann, “Dephasing in quantum dots: Quadratic coupling to acoustic phonons,” *Phys. Rev. Lett.* **93**, 237401 (2004).
- ³⁴P. Bertet, I. Chiorescu, G. Burkard, K. Semba, C. J. P. M. Harmans, D. P. DiVincenzo, and J. E. Mooij, “Dephasing of a superconducting qubit induced by photon noise,” *Phys. Rev. Lett.* **95**, 257002 (2005).
- ³⁵Y. J. Yan and S. Mukamel, “Eigenstate-free, Green function: Calculation of molecular absorption and fluorescence line shapes,” *J. Chem. Phys.* **85**, 5908 (1986).
- ³⁶Q. Peng, Y. P. Yi, Z. G. Shuai, and J. S. Shao, “Excited state radiationless decay process with Duschinsky rotation effect: formalism and implementation,” *J. Chem. Phys.* **126**, 114302 (2007).
- ³⁷H. Wang and M. Thoss, “Quantum Dynamical Simulation of Electron-Transfer Reactions in an Anharmonic Environment,” *J. Phys. Chem. A* **111**, 10369 (2007).
- ³⁸Y. Zhao and W. Z. Liang, “Charge transfer in organic molecules for solar cells: theoretical perspective,” *Chem. Soc. Rev.* **41**, 1075 (2012).
- ³⁹V. Chorošajev, T. Marčiulionis, and D. Abramavicius, “Temporal dynamics of excitonic states with nonlinear electron-vibrational coupling,” *J. Chem. Phys.* **147**, 074114 (2017).
- ⁴⁰Y. Wang, Y. Su, R. X. Xu, X. Zheng, and Y. J. Yan, “Marcus’ electron transfer rate revisited via a generalized Rice-Ramsperger-Kassel-Marcus theory with nonlinear environments,” *Chin. J. Chem. Phys.* **34**, 462 (2021).
- ⁴¹R. X. Xu, Y. Liu, H. D. Zhang, and Y. J. Yan, “Theory of quantum dissipation in a class of non-Gaussian environments,” *Chin. J. Chem. Phys.* **30**, 395 (2017).
- ⁴²R. X. Xu, Y. Liu, H. D. Zhang, and Y. J. Yan, “Theories of quantum dissipation and nonlinear coupling bath descriptors,” *J. Chem. Phys.* **148**, 114103 (2018).
- ⁴³Y. A. Yan, “Stochastic simulation of anharmonic dissipation. II. Harmonic bath potentials with quadratic couplings,” *J. Chem. Phys.* **150**, 074106 (2019).
- ⁴⁴C.-Y. Hsieh and J. Cao, “A unified stochastic formulation of dissipative quantum dynamics. II. Beyond linear response of spin baths,” *J. Chem. Phys.* **148**, 014104 (2018).
- ⁴⁵J. T. Hsiang and B. L. Hu, “Nonequilibrium nonlinear open quantum systems: Functional perturbative analysis of a weakly anharmonic oscillator,” *Phys. Rev. D* **101**, 125002 (2020).
- ⁴⁶J. T. Hsiang and B. L. Hu, “Fluctuation-dissipation relation from the nonequilibrium dynamics of a nonlinear open quantum system,” *Phys. Rev. D* **101**, 125003 (2020).
- ⁴⁷Y. J. Yan, “Theory of open quantum systems with bath of electrons and

- phonons and spins: Many-dissipaton density matrixes approach,” *J. Chem. Phys.* **140**, 054105 (2014).
- ⁴⁸R. X. Xu, H. D. Zhang, X. Zheng, and Y. J. Yan, “Dissipaton equation of motion for system-and-bath interference dynamics,” *Sci. China Chem.* **58**, 1816 (2015), Special Issue: Lemin Li Festschrift.
- ⁴⁹H. D. Zhang, R. X. Xu, X. Zheng, and Y. J. Yan, “Statistical quasi-particle theory for open quantum systems,” *Mol. Phys.* **116**, 780 (2018), Special Issue, “Molecular Physics in China”.
- ⁵⁰Y. Wang, R. X. Xu, and Y. J. Yan, “Entangled system-and-environment dynamics: Phase-space dissipaton theory,” *J. Chem. Phys.* **152**, 041102 (2020).
- ⁵¹Y. Wang and Y. J. Yan, “Quantum mechanics of open systems: Dissipaton theories,” *J. Chem. Phys.* **157**, 170901 (2022).
- ⁵²H. D. Zhang, R. X. Xu, X. Zheng, and Y. J. Yan, “Nonperturbative spin-boson and spin-spin dynamics and nonlinear Fano interferences: A unified dissipaton theory based study,” *J. Chem. Phys.* **142**, 024112 (2015).
- ⁵³Z. H. Chen, Y. Wang, R. X. Xu, and Y. J. Yan, “Correlated vibration-solvent effects on the non-Condon exciton spectroscopy,” *J. Chem. Phys.* **154**, 244105 (2021).
- ⁵⁴Z. H. Chen, Y. Wang, R. X. Xu, and Y. J. Yan, “Quantum dissipation with nonlinear environment couplings: Stochastic fields dressed dissipaton equation of motion approach,” *J. Chem. Phys.* **155**, 174111 (2021).
- ⁵⁵H. Risken, *The Fokker-Planck Equation, Methods of Solution and Applications*, Springer-Verlag, Berlin, 2nd edition, 1989.
- ⁵⁶R. X. Xu, B. L. Tian, J. Xu, and Y. J. Yan, “Exact dynamics of driven Brownian oscillators,” *J. Chem. Phys.* **130**, 074107 (2009).
- ⁵⁷J. J. Ding, Y. Wang, H. D. Zhang, R. X. Xu, X. Zheng, and Y. J. Yan, “Fokker-Planck quantum master equation for mixed quantum-semiclassical dynamics,” *J. Chem. Phys.* **146**, 024104 (2017).
- ⁵⁸H. Gong, Y. Wang, H. D. Zhang, R. X. Xu, X. Zheng, and Y. J. Yan, “Thermodynamic free-energy spectrum theory for open quantum systems,” *J. Chem. Phys.* **153**, 214115 (2020).
- ⁵⁹Y. Tanimura, “Reduced hierarchical equations of motion in real and imaginary time: Correlated initial states and thermodynamic quantities,” *J. Chem. Phys.* **141**, 044114 (2014).
- ⁶⁰H. Gong, Y. Wang, X. Zheng, R. X. Xu, and Y. J. Yan, “Nonequilibrium work distributions in quantum impurity system-bath mixing processes,” *J. Chem. Phys.* **157**, 054109 (2022).
- ⁶¹J. Hu, R. X. Xu, and Y. J. Yan, “Padé spectrum decomposition of Fermi function and Bose function,” *J. Chem. Phys.* **133**, 101106 (2010).
- ⁶²J. Hu, M. Luo, F. Jiang, R. X. Xu, and Y. J. Yan, “Padé spectrum decompositions of quantum distribution functions and optimal hierarchical equations of motion construction for quantum open systems,” *J. Chem. Phys.* **134**, 244106 (2011).
- ⁶³J. J. Ding, R. X. Xu, and Y. J. Yan, “Optimizing hierarchical equations of motion for quantum dissipation and quantifying quantum bath effects on quantum transfer mechanisms,” *J. Chem. Phys.* **136**, 224103 (2012).
- ⁶⁴H. Fan, H. Yuan, and N. Jiang, “New identities about operator Hermite polynomials and their related integration formulas,” *Sci. China Phys. Mech. Astron.* **54**, 2145 (2011).
- ⁶⁵Y. Wang, “Quantum Mechanics of Open Systems: Dissipaton Theory (in Chinese),” PhD Thesis, University of Science and Technology of China (2020), DOI:10.27517/d.cnki.gzkju.2020.000617; See also: <http://home.ustc.edu.cn/~wy2010/thesis.pdf>.
- ⁶⁶J. J. Ding, H. D. Zhang, Y. Wang, R. X. Xu, X. Zheng, and Y. J. Yan, “Minimum-exponents ansatz for molecular dynamics and quantum dissipation,” *J. Chem. Phys.* **145**, 204110 (2016).
- ⁶⁷Z. H. Chen, Y. Wang, X. Zheng, R. X. Xu, and Y. J. Yan, “Universal time-domain Prony fitting decomposition for optimized hierarchical quantum master equations,” *J. Chem. Phys.* **156**, 221102 (2022).
- ⁶⁸E. Wigner, “On the quantum correction for thermodynamic equilibrium,” *Phys. Rev.* **40**, 749 (1932).
- ⁶⁹Y. Liu, R. X. Xu, H. D. Zhang, and Y. J. Yan, “Dissipaton equation of motion theory versus Fokker-Planck quantum master equation,” *Chin. J. Chem. Phys.* **31**, 245 (2018).
- ⁷⁰A. O. Caldeira and A. J. Leggett, “Path integral approach to quantum Brownian motion,” *Physica A* **121**, 587 (1983).
- ⁷¹Q. Shi, L. P. Chen, G. J. Nan, R. X. Xu, and Y. J. Yan, “Efficient hierarchical Liouville space propagator to quantum dissipative dynamics,” *J. Chem. Phys.* **130**, 084105 (2009).
- ⁷²C. Jarzynski, “Equalities and inequalities: Irreversibility and the Second Law of Thermodynamics at the nanoscale,” *Ann. Rev. Cond. Matter Phys.* **2**, 329 (2011).
- ⁷³G. E. Crooks, “Entropy production fluctuation theorem and the nonequilibrium work relation for free energy differences,” *Phys. Rev. E* **60**, 2721 (1999).
- ⁷⁴P. Talkner and P. Hänggi, “The Tasaki-Crooks quantum fluctuation theorem,” *J. Phys. A: Math. Theor.* **40**, F569 (2007).
- ⁷⁵P. Talkner, E. Lutz, and P. Hänggi, “Fluctuation theorems: Work is not an observable,” *Phys. Rev. E* **75**, 050102 (2007).
- ⁷⁶S. Sakamoto and Y. Tanimura, “Open quantum dynamics theory for nonequilibrium work: Hierarchical equations of motion approach,” *J. Phys. Soc. Jpn.* **90**, 033001 (2021).
- ⁷⁷M. Esposito, U. Harbola, and S. Mukamel, “Nonequilibrium fluctuations, fluctuation theorems, and counting statistics in quantum systems,” *Rev. Mod. Phys.* **81**, 1665 (2009).
- ⁷⁸P. L. Du, Y. Wang, R. X. Xu, H. D. Zhang, and Y. J. Yan, “System-bath entanglement theorem with Gaussian environments,” *J. Chem. Phys.* **152**, 034102 (2020).
- ⁷⁹Y. Wang, Z. H. Chen, R. X. Xu, X. Zheng, and Y. J. Yan, “A statistical quasi-particles thermofield theory with Gaussian environments: System-bath entanglement theorem for nonequilibrium correlation functions,” *J. Chem. Phys.* **157**, 044012 (2022).
- ⁸⁰M. O. Scully and M. S. Zubairy, *Quantum Optics*, Cambridge University Press, Cambridge, 1997.